Analysis of Binding Interaction between Bovine Serum Albumin and the Cobalt(II) Complex with Salicylaldehyde-2-phenylquinoline-4-carboylhydrazone

Hong-yan Liu,[a] Zhi-hong Xu,[b] Xiao-hui Liu,[a] Pin-xian Xi,[a] and Zheng-zhi Zeng*,[a]

[a] *College of Chemistry and Chemical Engineering and State Key Laboratory of Applied Organic Chemistry, Lanzhou University; Lanzhou 730000, P. R. China: and* [b] *College of Chemistry and Chemical Engineering, Xuchang University; Xuchang 461000, P. R. China.* Received May 9, 2009; accepted July 10, 2009; published online August 10, 2009

The interaction between bovine serum albumin (BSA) and the cobalt(II) complex with salicylaldehyde-2-phenylquinoline-4-carboylhydrazone (Co-SPC) was investigated using fluorescence spectroscopy, UV absorption, and circular dichroism (CD) under simulated physiologic conditions for the first time. Fluorescence data and UV absorption spectra revealed that the intrinsic fluorescence of BSA was strongly quenched by Co-SPC in terms of a static quenching process at a lower concentration of the complex and a combined quenching process at a higher concentration of the complex. Binding constants and binding sites were evaluated. The average binding distance between Co-SPC and BSA was obtained (2.28 nm) on the basis of Förster's theory. The thermodynamic parameters indicated that hydrophobic force played a major role in the binding. The binding of Co-SPC to BSA leads to changes in the conformation of BSA according to synchronous fluorescence spectra and CD data.

Key words bovine serum albumin; co-complex; fluorescence quenching; circular dichroism

Serum albumins, bovine serum albumin (BSA) and human serum albumin (HSA), are most widely studied abundant proteins in plasma.[1,2] As the major soluble protein constituents of the circulatory system, they contribute to colloid osmotic blood pressure and are chiefly responsible for the maintenance of blood pH.[3] They also are known to bind a variety of biologic probe molecules. They have a great affinity for fatty acids, hematin, bilirubin, *etc.*[4] Many drugs, including anticoagulants, tranquilizers, and general anesthetics, are transported in the blood while bound to albumin. The nature and magnitude of drug–albumin interactions significantly influence the pharmacokinetics of drugs, and the binding parameters are useful in studying protein–drug binding as they greatly influence absorption, distribution, metabolism, and excretion properties of typical drugs.[5]

Schiff bases play a major role in bioinorganic chemistry as they exhibit remarkable biological activity. They have a wide range use in biology and many of their ramifications have been used as antifebrile, pain, and antirheumatism agents. The acid hydrazides R–CO–NH–NH_2, a class of Schiff base, their corresponding aroylhydrazones, R–CO–NH–N=CH–R′, and the dependence of their mode of chelation with transition metal ions present in the living system have been of significant interest. The coordination compounds of aroylhydrazones have been reported to act as enzyme inhibitors[6] and are useful due to their pharmacologic applications.[7] It was demonstrated that 4-quinolinecarboxylic acid amides and hydrazides, substituted at position 2, exhibit pronounced anti-inflammatory and analgesic activity with low toxicity,[7,8] and such drugs were reported to have better pharmaceutical effects. However, the binding interaction between the metal complexes and BSA has not been reported, and therefore the study of their interaction with BSA is important. Molecular interactions are often monitored using different optical techniques. Fluorescence spectroscopy is perhaps the most important technique to study the interaction of probes with proteins because of the high sensitivity of the technique and the relative ease of its use. Molecular interactions of different fluorophores such as 3-hydroxy flavone,[9] 1-anilino-8-naphthalene sulfonate,[10] diethylamino coumarin,[11] and quercetin[12] with BSA and HSA have been studied by different groups, and different compounds have been used as probes such as dyes,[13] drugs,[14] and metal complexes.[15]

In the present work, salicylaldehyde 2-phenylquinoline-4-carboylhydrazone (H_2L) and its cobalt(II) complex $[Co(HL)(H_2O)_3]\cdot NO_3$ were synthesized and characterized. The binding of cobalt(II) complex with salicylaldehyde-2-phenylquinoline-4-carboylhydrazone (Co-SPC) to BSA was studied under simulated physiologic conditions. Efforts were made to investigate the quenching mechanism, binding constants, binding sites, binding mode, binding location, and the effects of Co-SPC on the conformation of BSA.

Experimental

Materials All starting materials were of analytical grade and double-distilled water was used throughout the experiments. BSA, purchased from Shanghai Chemical Reagent Company, was dissolved in buffer solution, pH 7.4, and BSA stock solution (1.50×10^{-5} mol l^{-1}) was kept in the dark at 0—4 °C. Tris/HCl buffer solution (pH 7.4) and NaCl solution (0.1 mol l^{-1}) were prepared to maintain the ionic strength. H_2L (Fig. 1) and its cobalt(II) complex were synthesized according to the literature.[7] Its stock solution (5.00×10^{-4} mol l^{-1}) was prepared in absolute methanol.

Apparatus and Methods Fluorescence spectrum scans were measured with an F-4500 fluorophotometer (Hitachi, Japan), and the results of fluorometric titration experiments at different temperatures were recorded on an LS-55 fluorophotometer (U.S.A.) equipped with a thermostat bath.

In fluorometric titration experiments, 2.0 ml of operating solution (BSA 1.50×10^{-6} mol l^{-1}, NaCl 0.10 mol l^{-1}, pH 7.4) was titrated by successive additions of a 5.00×10^{-4} mol l^{-1} methanol stock solution of Co-SPC. Titrations were done using a microinjector, and the fluorescence intensity was measured (excitation at 280 nm and 2.5 nm slit widths). The experiments were measured at three temperatures (286, 298, 310 K). The temperature of

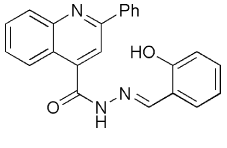

Fig. 1. Structure of Salicylaldehyde-2-phenylquinoline-4-carboylhydrazone

* To whom correspondence should be addressed. e-mail: zengzhzh@yahoo.com.cn

samples was maintained with recycled water. Fluorescence spectrum scans were recorded at room temperature using methods similar to those in titration experiments.

In site maker competitive experiments, the proportion of BSA and phenylbutazone (PB), flufenamic acid (FA), and digitoxin (Dig) was kept at 1 : 1 by adding PB, FA, and Dig solution (1×10^{-3} mol l^{-1}) to 2.0 ml of operating BSA solution (1.50×10^{-6} mol l^{-1}), and then titrated by methanol stock solution of Co-SPC, similar to the methods used in fluorometric titration experiments.

Synchronous fluorescence spectra were obtained by scanning the excitation and emission monochromator simultaneously at 5 nm slit widths. The wavelength interval ($\Delta\lambda$) was fixed individually at 15 and 60 nm, at which the spectrum only shows the spectroscopic behavior of the tyrosine and tryptophan residues of BSA.

A Carry 100 UV–vis spectrophotometer (Varian, U.S.A.) equipped with 1.0 cm quartz cells was used for scanning the UV spectrum in the wavelength range from 200 to 500 nm. The Tris/HCl buffer solution was used as a reference solution.

Circular dichroism (CD) measurements were performed on a Jasco-20 automatic recording spectropolarimeter (Japan) in cells of 1 mm path length at room temperature. CD spectra (200—300 nm) were recorded at a BSA concentration of 1.50×10^{-6} mol l^{-1}, and the results were taken as molar ellipticity ([θ]) in deg cm^2 dmol^{-1}. The α-helical content of BSA was calculated from the [θ] value at 222 nm using the equation[16] % helix$=\{(-[\theta]_{222}-2340)/30300\}\times100$.

Results and Discussion

Quenching Mechanism of BSA Fluorescence by Co-SPC A useful feature of the intrinsic fluorescence of proteins is the high sensitivity of tryptophan and its local environment. Changes in the emission spectra of tryptophan are common in response to protein conformational transitions, subunit associations, substrate binding, or denaturation.[17] Therefore the intrinsic fluorescence of proteins can provide considerable information on their structure and dynamics and is often utilized in the study of protein folding and association reactions.

The effect of Co-SPC on tryptophan residue fluorescence intensity of BSA is shown in Fig. 2, which indicates the fluorescence emission of BSA with different amounts of Co-SPC following excitation at 280 nm. BSA exhibits strong fluorescence emission at 346 nm. Under the same experimental conditions, the fluorescence intensity of Co-SPC was very weak, and thus the effect of the maximum fluorescence intensity could be ignored. As the data show, the fluorescence intensity of BSA decreased with the increasing concentration of Co-SPC, which indicates that there were interactions between Co-SPC and BSA.

Figure 3 shows the UV absorption spectra of BSA in the presence and absence of Co-SPC. The absorption intensity of BSA was enhanced as Co-SPC increased, and there was a distinct blue shift of the Co-SPC–BSA spectrum (from 278 to 270 nm). As is well known, dynamic quenching only affected the excited state of fluorophores but did not change the absorption spectrum. However, the formation of a nonfluorescence ground state of Co-SPC induced a change in the absorption spectrum of fluorophores, and therefore the possible quenching mechanism of BSA by Co-SPC is a static quenching process.[18]

To elucidate further the quenching mechanism, fluorescence quenching data were analyzed with the Stern–Volmer Eq. 1 and the modified Stern–Volmer Eq. 2.[19]

$$F_0/F=1+K_q\tau_0[Q]=1+K_{sv}[Q] \quad (1)$$

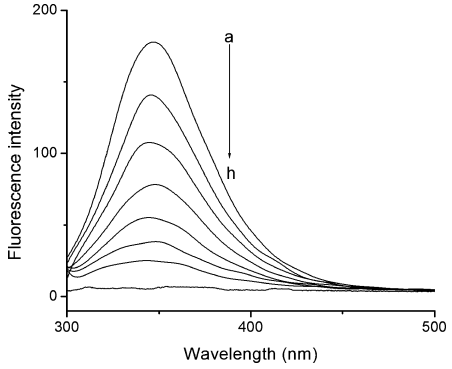

Fig. 2. Fluorescence Spectra of BSA after Excitation at 280 nm at pH 7.4 and 286 K with Various Amounts of Co-SPC: (a)—(g), Respectively, BSA 1.50×10^{-6} mol l^{-1} in the Presence of 0.00, 0.75, 1.50, 2.50, 3.75, 5.00, and 6.25×10^{-6} mol l^{-1} of Co-SPC, (h), 6.25×10^{-6} mol l^{-1} of Co-SPC
Slits, 2.5 nm/2.5 nm.

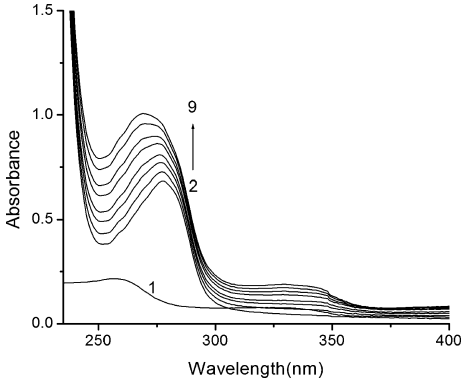

Fig. 3. UV Absorption Spectra of BSA in the Presence of Co-SPC: (2)—(9), Respectively, BSA 1.50×10^{-5} mol l^{-1} in the Presence of 0, 1.25, 2.50, 3.75, 5.00, 6.25, 7.5, and 8.75×10^{-6} mol l^{-1} of Co-SPC, (1), 8.75×10^{-6} mol l^{-1} of Co-SPC

$$\frac{F_0}{F_0-F}=\frac{1}{[Q]}\cdot\frac{1}{fK}+\frac{1}{f} \quad (2)$$

where F and F_0 are the relative fluorescence intensities in the presence and absence of quencher, respectively, [Q] is the concentration of quencher, K_{sv} is the Stern–Volmer quenching constant, k_q is the bimolecular quenching rate constant, τ_0 is the average bimolecular lifetime in the absence of quencher evaluated at about 10^{-8} s,[20] f is the fraction of the initial fluorescence which is accessible to the quencher, and K is the modified Stern–Volmer quenching constant.

The Stern–Volmer curves of BSA–Co-SPC at different temperatures are shown in Fig. 4. The Stern–Volmer plot follows a linear relation at low concentrations of Co-SPC but exhibits an upward curve when the concentration of Co-SPC is greater than 2.5 μM. This suggests that the quenching type was probably single quenching (static or dynamic quenching) at lower Co-SPC concentrations. But at higher Co-SPC concentrations, combined quenching (both staticand dynamic) would occur. Thus the positive deviation is due to the presence of a quencher molecule in the same solvent cage as the fluorophores at the moment of excitation. Some of the excited states are deactivated almost instantaneously after the formation of the complex because Co-SPC molecules appear randomly in proximity to BSA fluorophores at the time of

their excitation.[21)]

The plots of $F_0/(F_0-F)$ for BSA *versus* 1/[Q] in the entire concentration range of Co-SPC based on Eq. 2 exhibit good linearity (Fig. 5). The values for f at 286 K, 298 K, and 310 K indicate that 67.51%, 68.65%, and 69.50%, respectively, of the total fluorophores of excited BSA was accessed by Co-SPC.

To clarify the quenching mechanism, the following points were examined:

1) The K_{sv} values decrease with an increase in temperature for static quenching, but the reverse effect would be observed for dynamic quenching.[22,23)] In this study, the values of K_{sv} (Table 1) were found to increase with higher temperature, indicating that dynamic quenching actually occured in the quenching process.

2) The values for k_q (Table 1) are three orders of magnitude greater than the maximum diffusion collision quenching rate constant (2.0×10^{10} l mol^{-1} s^{-1}) for a variety of quenchers with biopolymers.[24)] This indicates that static quenching occured in the quenching process.

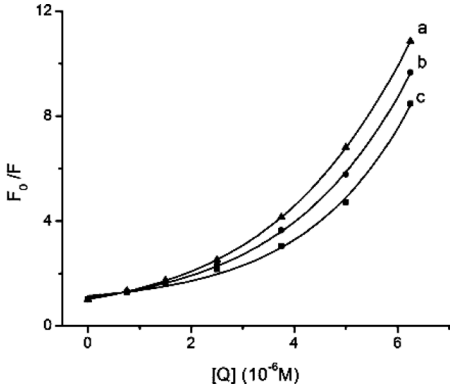

Fig. 4. Plots of F_0/F for BSA against [Q] of Co-SPC from 0 to 6.25×10^{-6} mol l^{-1} at (a) 310 K, (b) 298 K, and (c) 286 K

BSA = 1.5×10^{-6} mol l^{-1}, λ_{ex} = 280 nm, λ_{em} = 347 nm, and pH = 7.4.

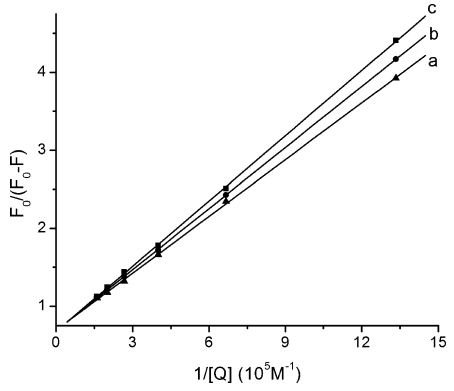

Fig. 5. Modified Stern–Volmer Plots for the BSA–Co-SPC System at (a) 310 K, (b) 298 K, and (c) 286 K

3) The Stern–Volmer slope is expected to depend on the concentration of the donor in a static quenching process.[25)] Analysis of Stern–Volmer plots at different concentrations of BSA was performed. Plots of F_0/F for BSA *versus* [Q] of Co-SPC at different concentrations of BSA with Co-SPC concentrations of less than 2.5 μM exhibited good linearity (data not shown). The results are presented in Table 1, which indicate that K_{sv} decreases with increasing concentrations of BSA. This evidence suggests that the fluorescence quenching process of BSA at low concentrations (less than 2.5 μM) of Co-SPC may mainly be governed by a static quenching mechanism. This is an indication that quenching occurs *via* the formation of the complex.

According to all the evidence obtained, we can conclude that single static quenching occured at low concentrations of Co-SPC but combined quenching occured at higher concentrations of Co-SPC.

Binding Constant and Binding Sites The apparent binding constant, K_A and binding sites n can be evaluated using the following equation[26)]:

$$\log\frac{F_0-F}{F}=n\log K_A-n\log\left(\frac{1}{[Dt]-(F_0-F)[Pt]/F_0}\right) \quad (3)$$

where F_0 and F are the fluorescence intensities before and after the addition of the quencher, respectively, and [Dt] and [Pt] are the total quencher concentration and the total protein concentration, respectively. Based on the plot of $\log(F_0-F)/F$ *versus* $\log(1/([Dt]-(F_0-F)[Pt]/F_0))$ (Fig. 6), the number of binding sites n and binding constant K_A can be obtained, as presented in Table 2.

Thermodynamic Parameters and Type of Binding Forces There are four types of interaction force which could play a role in ligand binding to proteins: hydrogen bonds; vander Waals forces; electrostatic interactions; and hydrophobic interactions.[27)] Considering the dependence of the binding constant K_A (Co-SPC–BSA) on temperature, a

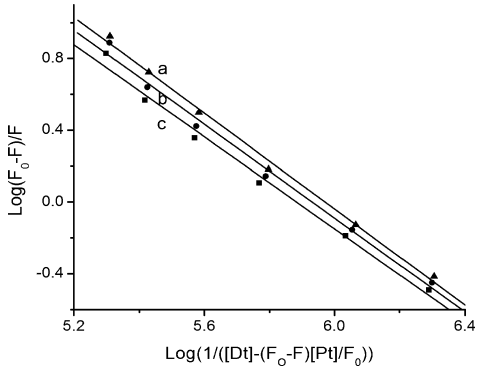

Fig. 6. Plots of $\log(F_0-F)/F$ *vs.* $\log(1/([Dt]-(F_0-F)[Pt]/F_0))$ for the BSA–Co-SPC System at (a) 310 K, (b) 298 K, and (c) 286 K

Table 1. Fluorescence Quenching Constants of Co-SPC–BSA System at Different Temperatures and Different Concentrations of BSA

T(K)	K_q ($\times10^{13}$ l·mol^{-1}·s^{-1})	K_{sv} ($\times10^5$ l·mol^{-1})	T(K)	[BSA] ($\times10^{-6}$ M)	K_{sv} ($\times10^5$ l·mol^{-1})
286	4.43	4.43		1.5	4.67
298	4.67	4.67	298		
310	4.96	4.96		2.25	2.95

Table 2. Binding Constants K_A, Numbers of Binding Sites n and Thermodynamic Parameters for the Co-SPC–BSA System

T (K)	K_A ($\times 10^5$ l·mol^{-1})	n	R	ΔG (kJ·mol^{-1})	ΔH (kJ·mol^{-1})	ΔS (J·mol^{-1}·K^{-1})
286	7.98	1.26	0.996	−32.31		137.83
298	9.11	1.27	0.995	−33.99	7.11	137.92
310	10.18	1.29	0.998	−35.56		137.94

R is the correlation coefficient.

thermodynamic process was considered to be responsible for the formation of the complex. Thermodynamic parameters for a binding interaction can be used as major evidence for the nature of intermolecular forces.[25] Among these parameters, the free energy change ΔG reflects the possibility of reaction, and the enthalpy change ΔH and entropy change ΔS are the main evidence for determining acting forces. To obtain such information, the thermodynamic parameters were calculated from the Van't Hoff equation. If $\Delta H \approx 0$, $\Delta S > 0$, the main force is a hydrophobic interaction; if $\Delta H < 0$, $\Delta S > 0$, the main force is an electrostatic effect; if $\Delta H < 0$, $\Delta S < 0$, Van der Waals and hydrogen bond interactions play major roles in the reaction.[28] The values of ΔG, ΔH, and ΔS were calculated according to the data on the binding constant K_A at 286 K, 298 K, and 310 K using Eqs. 4—6.

$$\Delta G = -RT \ln K \tag{4}$$

$$\ln \frac{K_{A2}}{K_{A1}} = \left[\frac{1}{T_1} - \frac{1}{T_2} \right] \frac{\Delta H}{R} \tag{5}$$

$$\Delta G = \Delta H - T\Delta S \tag{6}$$

The values of thermodynamic parameters are shown in Table 2, where the negative sign for ΔG indicates the spontaneity of the binding of Co-SPC with BSA. ΔH is a small positive value and ΔS is a positive value, indicating that the main binding force between Co-SPC and BSA is a hydrophobic interaction.

Energy Transfer from BSA to Co-SPC According to the Förster nonradiative energy-transfer theory,[29] the efficiency of energy transfer is E, the critical distance for 50% energy transfer is R_0, and the actual distance of separation is r. These values were calculated using Eqs. 7—9:

$$E = 1 - \frac{F}{F_0} = \frac{R_0^6}{R_0^6 + r^6} \tag{7}$$

$$R_0^6 = 8.78 \times 10^{-25} \kappa^2 n^{-4} \phi_{Trp} J \tag{8}$$

where κ^2 is the orientation factor, ϕ_{Trp} is the quantum yield of the donor tryptophan in the absence of acceptor, n is the refractive index of the medium intervening between the donor and acceptor, and J is the spectral overlap integral defined by Eq. 9:

$$J = \sum F(\nu)\varepsilon(\nu)\nu^{-4}\Delta\nu \Big/ \sum F(\nu)\Delta\nu \tag{9}$$

where $F(\nu)$ is the fluorescence intensity of the donor, $\varepsilon(\nu)$ is the molar extinction coefficient of the acceptor in units of M^{-1} cm^{-1}, and ν is the frequency in cm^{-1}. The fluorescence emission spectrum of BSA and the UV absorption spectrum of Co-SPC are shown in Fig. 7, which shows that they have some overlap. The value of J was 1.28106×10^{-14} cm^3·l·mol^{-1}. κ^2 taken as 2/3. n taken as 1.36.[29] ϕ_{Trp} was determined in the study to be 0.15.[30] With use of the values of J, κ^2, n, and ϕ_{Trp}, the R_0 value was calculated to be 2.65 nm. The efficiency of energy transfer E was 0.41187. The actual distance r was 2.82 nm. BSA has two tryptophan residues: Trp-212 is located in a hydrophobic fold and the additional tryptophan (Trp-134) is located on the surface of the molecule. In this study, Co-SPC was probably bound to the Trp-212 residue mainly through the hydrophobic interaction according to the thermodynamic results. However, an interaction between Trp-134 and Co-SPC cannot be ruled out, and therefore the distance calculated here is actually the average distance between Co-SPC and the two tryptophan residues in BSA. The energy transfer from BSA to Co-SPC occurs with very high probability.

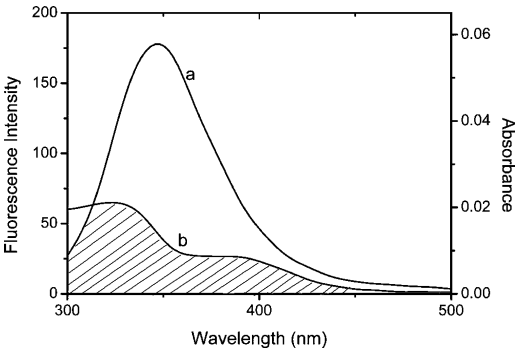

Fig. 7. Overlap of Fluorescence Spectra of BSA and UV Absorption Spectrum of Co-SPC

(a) Fluorescence spectrum of BSA (1.50×10^{-6} mol l^{-1}); (b) UV absorption spectrum of Co-SPC (1.50×10^{-6}mol l^{-1}).

Identification of Binding Location on BSA HSA has a limited number of binding sites. The principal regions of ligand-binding sites of albumin are located in hydrophobic cavities in subdomains IIA and IIIA. The IIIA subdomain is the most active in accommodating many ligands.[31] It has been reported that specific drug-binding sites resembling those in humans probably exist in bovines.[32] Thus site marker competitive experiments were carried out on the hypothesis that BSA contains binding sites for PB, FA, and Dig, which specifically bind to known sites of HSA: PB is a characteristic marker for site I; FA for site II; and Dig for site III.[33] According to the modified Stern–Volmer equation (Eq. 2), the fluorescence data were used to obtain the values of modified binding constant K (4.52×10^5 l/mol, $R = 0.998$; 2.29×10^5 l/mol, $R = 0.997$; 4.48×10^5 l/mol, $R = 0.999$ for PB, FA, and Dig, respectively, at 298 K). The results indicate that the binding of Co-SPC to BSA was affected by adding the drugs, and the addition of FA had the most marked effect. This evi-

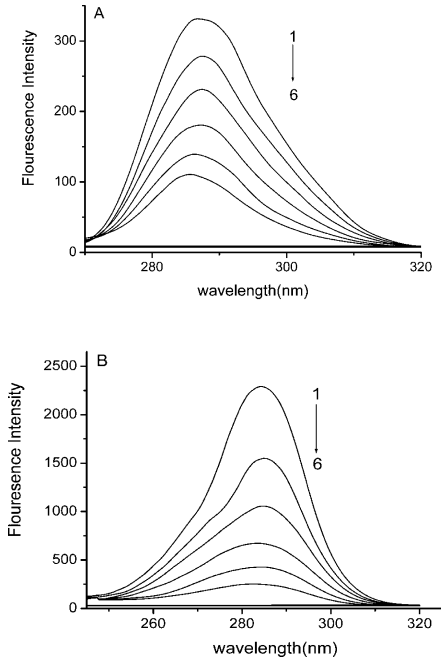

Fig. 8. Synchronous Fluorescence Spectra of BSA

(A) $\Delta\lambda=15$ nm; (B) $\Delta\lambda=60$ nm; (1)—(6), respectively, BSA 1.50×10^{-6} mol l^{-1} in the presence of 0.00, 0.75, 1.50, 2.50, 3.75, and 5.00×10^{-6} mol l^{-1} of Co-SPC. Slits, 5 nm/5 nm.

dence suggests that the binding of Co-SPC to BSA is the same as that of FA to HSA, *i.e.*, BSA probably contains a specific drug-binding site corresponding to site II on the human albumin molecule.

Effects of Co-SPC on BSA Conformation Synchronous fluorescence spectra can be used to analyze changes in BSA because the shift in the position of the maximum emission wavelength corresponds to changes in the polarity around the chromophore molecule. When $\Delta\lambda=15$ nm, a spectrum characteristic of protein tyrosine residues is observed, and when $\Delta\lambda=60$ nm, a spectrum characteristic of protein tryptophan residues is observed. The environment of amino acid residues was studied by measuring the possible shift in the wavelength emission maximum λ_{max}. When the concentration of Co-SPC increased by titration, synchronous spectroscopy was performed at $\Delta\lambda=15$ and 60 nm. As shown in Fig. 8, the quenching of the fluorescence intensity of tryptophan residues is stronger than that of the tyrosine residues, suggesting that tryptophan residues contribute greatly to the quenching of intrinsic BSA fluorescence. Moreover, a slight blue shift of the maximum emission wavelength of tyrosine residues was observed upon the addition of complex, whereas the emission maximum of tryptophan remained unchanged, which indicates that the conformation of BSA changed and the hydrophobicity around the tyrosine residues increased. However, the microenvironment around the tryptophan residues did not undergo obvious changes during the binding process.[34)]

Further experiments were carried out on the CD spectra to verify the binding process. As Fig. 9 shows, the CD spectra of BSA exhibited two negative bands in the UV region at 208 and 222 nm, characteristic of the α-helical structure of the protein.[16)] The binding of Co-SPC to BSA caused a decrease in band intensity in the ultra-UV CD, clearly indicating a decrease in the α-helical content in the protein. The calculated results exhibited a reduction of α-helix structures from 62.3 to 56.8% at the molar ratio Co-SPC/BSA of 1 : 1. The marked decrease probably occured because of the strong interaction between Co-SPC and BSA, which can be confirmed by the value of the binding constant K_A. This decreased helicity suggests that the binding of Co-SPC with BSA induces a slight unfolding of the constitutive polypeptides of the protein, which results in a conformational change in the protein which increased the exposure of some hydrophobic regions that were previously covered.

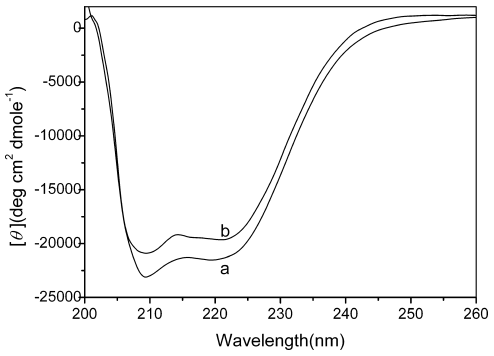

Fig. 9. CD Spectra of the BSA–Co-SPC System at Room Temperature (in Cells of 1 mm Path Length)

(a) BSA 1.50×10^{-6} mol l^{-1}; (b) BSA 1.50×10^{-6} mol l^{-1}+Co-SPC 1.50×10^{-6} mol l^{-1}.

Conclusion

We studied the interaction of $[Co(HL)(H_2O)_3]\cdot NO_3$ with a model transport protein, BSA. The binding behavior of the complex was first investigated under simulatied physiologic conditions. The experimental results showed that the intrinsic fluorescence of BSA was quenched by a combined quenching mechanism, and Co-SPC bound to BSA *via* hydrophobic interaction. The binding site corresponds to site II on the human albumin molecule. Co-SPC can therefore be deposited and transported by albumin. The results also indicate that the binding of Co-SPC to BSA induces a conformational change in BSA, which was confirmed by the synchronous fluorescence and quantitative analysis data of the CD spectrum.

The biological significance of these results are clear since serum albumin serves as a carrier molecule for multiple drugs, and the interactions of metal complexes of Schiff base drugs and BSA were not reported previously. This report will be significant in pharmacology and clinical medicine.

References

1) Carter D. C., Chang B., Ho J. X., Keeling K., *Eur. J. Biochem.*, **226**, 1049—1052 (1994).
2) Brown J. R., Shockley P., *Lipid-Protein Interactions*, **1**, 25—68 (1982).
3) Tan F., Guo M., Yu Q. S., *Spectrochim. Acta A*, **61**, 3006—3012 (2005).
4) Reed R. G., *J. Biol. Chem.*, **252**, 7483—7487 (1997).
5) Zsila F., Bikádi Z., Simonyi M., *Biochem. Pharmacol.*, **65**, 447—456 (2003).
6) Dilworth J. R., *Coord. Chem. Rev.*, **21**, 29—62 (1976).
7) Xu Z. H., Chen F. J., Xi P. X., Liu X. H., Zeng Z. Z., *J. Photochem. Photobiol. A*, **196**, 77—83 (2008).
8) Mliyutin A. V., Amirova L. R., Kolla V. E., *Pharm. Chem. J.*, **32**, 422—424 (1998).
9) Guharay J., Sengupta B., Sengupta P. K., *Proteins Struct. Funct.*

Genet., **43**, 75—81 (2001).
10) Nerli B., Pico G., *Int. Physiol. Biochem. Biophys.*, **102**, 5—8 (1994).
11) Nag A., Bhattacharya K., *Chem. Phys. Lett.*, **169**, 12—16 (1990).
12) Sengupta B., Sengupta P. K., *Biopolymers*, **72**, 427—434 (2003).
13) Baptista M. S., Indig G. L., *J. Phys. Chem. B*, **102**, 4678—4688 (1998).
14) Romanini D., Avalle G., Farruggia B., *Chem. Biol. Interact.*, **115**, 247—260 (1998).
15) Jin Y. J., Li W. L., Wang Q. R., *Biochem. Biophys. Res. Commun.*, **177**, 474—479 (1991).
16) Chen Y. H., Yang J. T., Martinez H. M., *Biochemistry*, **11**, 4120—4131 (1972).
17) Sulkowska A., *J. Mol. Struct.*, **616**, 227—232 (2002).
18) Zhang X. W., Zhao F. L., Li K. A., *Chem. J. Chin. Univ.*, **20**, 1063—1067 (1999).
19) Lehrer S. S., *Biochemistry*, **10**, 3254—3263 (1971).
20) Lakowicz J. R., Weber G., *Biochemistry*, **12**, 4171—4179 (1973).
21) Boaz, H., Rollefson, G. K., *J. Am. Chem. Soc.*, **72**, 3435—3443 (1950).
22) Huang Y. M., Zhang Z. J., Zhang D. J., *Talanta*, **53**, 835—841 (2001).
23) Qian L. H., Wang X. L., Tu Z. H., *Acta Pharmacol. Sin.*, **22**, 847—850 (2001).
24) Jiang C. Q., Gao M. X., He J. X., *Anal. Chim. Acta*, **452**, 185—189 (2002).
25) Li D. J., Zhu J. F., Jin J., *J. Photochem. Photobiol. A*, **189**, 114—120 (2007).
26) Bi S. Y., Ding L., Tian Y., *J. Mol. Struct.*, **703**, 37—45 (2004).
27) Cui F. L., Wang J. L., Cui Y. R., Li J. P., *Anal. Chim. Acta*, **571**, 175—183 (2006).
28) Ross P. D., Subramanian S., *Biochemistry*, **20**, 3096—3102 (1981).
29) Horrocks W. De W., Collier W. E., *J. Am. Chem. Soc.*, **103**, 2856—2862 (1981).
30) Liu X. H., Xi P. X., Chen F. J., Xu Z. H., Zeng Z. Z., *J. Photochem. Photobiol. B*, **92**, 98—102 (2008).
31) Sudlow G., Birkett D. J., Wade D. N., *Mol. Pharmacol.*, **12**, 1052—1061 (1976).
32) Kosa T., Maruyama T., Dtagiri M., *Pharm Res.*, **14**, 1607—1612, (1997).
33) He W. Y., Li Y., Xue C. X., *Bioorg. Med. Chem.*, **13**, 1837—1845 (2005).
34) Klajnert B., Bryszewska M., *Bioelectrochemistry*, **55**, 33—35 (2002).